INTERNATIONAL JOURNAL OF SOFTWARE ENGINEERING AND COMPUTER SYSTEMS
E-ISSN: 2180-0650
VOLUME 10, ISSUE 2, 2024, pp. 85 – 102
DOI: https://doi.org/10.15282/ijsecs.10.2.2024.8.0126

RESEARCH ARTICLE

An Integrated UAV-based Observer Platform Hybridising Online Fuzzy Classifier

Wan Isni Sofiah Wan Din[1], Loo Chen Wei[1], Wenhao Chen[2*], and Azlee Zabidi[1]

[1] Faculty of Computing, Universiti Malaysia Pahang, 26600 Pahang, Malaysia
[2] School of Electrical and Electronic Engineering, Universiti Sains Malaysia, 14300 Penang, Malaysia

ABSTRACT - Intelligent system-assisted UAV-based observer platforms could achieve various complex observing tasks over traditional methods. However, due to the complexity of their algorithms, UAV's first-flight route is still challenging to deploy quickly and minimise energy consumption in an emergency. Another challenge is that the UAV-based observer platform severely requires an efficient classifier with high processing speed for higher observing efficiency. As the first research objective, this paper artificially evaluated seven UAV first-flight routes by simulation and real-world flighting environments to identify one proper first-flight route that could be deployed quickly. Secondly, a new integrated UAV-based observer platform, including a new three-colour channel-based online fuzzy classifier, is proposed for quickly detecting abnormal objectives in practical observing tasks. Simulation and real-world flighting experiments identified that the square helix with smooth turn consumes the most miniature battery and can cover the observing area among seven different first-flight routes. The results also proved the proposed integrated observer platform's feasibility in detecting abnormal objectives while UAVs fly in a real-time, real-world environment. Most importantly, the proposed observer platform has good interpretability because it employs an actual image stream to train its classifier during flighting.

ARTICLE HISTORY

Received	:	29 December 2022
Revised	:	20 August 2024
Accepted	:	10 December 2024
Published	:	30 December 2024

KEYWORDS

Unmanned Aerial Vehicle
First Flight Route
Energy Consumption
Fuzzy Classifier
Online Learning

1.0 INTRODUCTION

Before the invention of the Unmanned Aerial Vehicle (UAV), also named the drone [1], helicopters were tools primarily used for terrain surveillance. A licensed pilot can only operate it, and its flight has high operation and manufacturing costs. Primarily, it is unsafe in bad weather conditions. Compared to helicopters, UAVs are much cheaper to manufacture and operate than helicopters. Besides, it is easy to use and develop [2]. One significant advantage is that it can fly to indeterminate hazardous areas for ground inspections, meaning no personal safety is at risk [3]. Therefore, the invention of UAVs as an alternative to helicopters has brought considerable gains to the market.

Unlike helicopters and other aircraft that require much fuel to sustain long flights, UAVs are primarily designed for efficiency and convenience. In today's intelligent industry 4.0 age [4], the UAV can be significantly applied in big smart cities [5] to protect city dweller health from some diseases [6]. Therefore, the method combining the efficient UAV and intelligent system abstracts the focus of the research. On the one hand, energy efficiency has always been a critical industry concern. Many reasons limit the energy efficiency of a UAV [7], such as external environmental disturbances (weather and wind) and internal issues (UAV's weight, payload, battery type, and flight speed). Understandably, this problem is exacerbated when flying first in unknown and unobstructed areas. Therefore, determining a practical and easy-to-control first flight route is crucial to observing unknown barrier-free areas [8]. On the other hand, intelligent system-assisted UAV not only has better recognition ability to abnormal objectives than people, but also intelligent UAV could be deployed for more complex working environment, that also means deploying intelligent systems on UAVs is one indispensable topic in today's intelligent era. In sum, this paper will achieve the following two objectives:

1) To identify one optimal first flight route for UAV,
2) To propose an intelligent UAV platform for detecting abnormal objectives.

This research will first analyse and determine a practical UAV first-flight route that can be easily used for the first-flight mission in barrier-free areas with minimal energy and maximise area coverage. Moreover, this paper will propose a new powerful online observer platform by employing a unique online fuzzy classifier based on one EDA (Empirical Data Analytics) technique [9, 10], allowing the observer platform to run in real time. In sum, this paper's contribution can be summarised in the following three:

1) Proposing an integrated UAV-based intelligent observer platform,
2) Determining one optimised first flight route while minimising UAV energy consumption,
3) Proposing an EDA-based online fuzzy classifier to capture abnormal objectives.

***CORRESPONDING AUTHOR | W. Chen** | ✉ chenwh@student.usm.my

The rest of this paper is organised as follows: Section II (RELATED WORKS) will review some critical references as the fundamentals of developing the proposed integrated UAV-based Observer Platform. Section III (METHODS AND MATERIAL) presents the overall methodology. Section III (RESULTS AND DISCUSSION) presents the experimental results, and Section IV (CONCLUSIONS) will summarise this research.

2.0 RELATED WORKS

First, to deal with the UAV flight routes problem, the research [11] proposed an energy-efficient route planning algorithm for UAVs, and they noticed that filtering and choosing the best route to deploy to that specific area is one problem. The authors [12] determined the optimum UAV flight route for disaster areas. They categorised two disaster areas: distributed and centralised areas. They calculated energy utilisation and paired the optimum UAV flight route [13], as Figures 1 and 2 showed. Their results pointed to using quad-copters UAVs rather than winged drones because they are more manoeuvrable and more accessible to deploy. Depending on their flight routes, O-path and Rectangular-path will cover the edges of the area but leave a massive gap within the area, while the Zig-Zag path and S-path cover most of the area to reduce the gaps, but with O-path Compared to Rectangle-path, Zig-Zag and S-path are not efficient in execution time. There is a problem with the steering angle of the Zig-Zag path. The larger the turning angle, the more pronounced the gap between the tracks. In contrast, the smaller the turning angle, the longer the flight time.

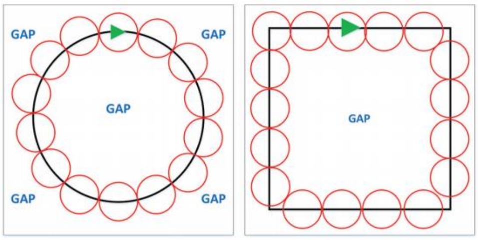

Figure 1. O-Path and Rectangular-Path

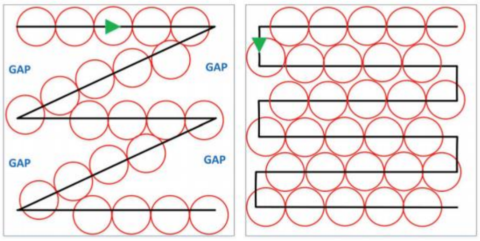

Figure 2. Zigzag-Path and S-Path

Table 1 summarises the above routes. For distributed area patterns (floods, hurricanes, and landslides), UAVs need longer flight times to scan the area. Therefore, the S-path is the optimal flight path for distributed mode, as the UAV can cover most of the area without gaps. For concentrated area patterns, such as earthquakes, volcanic eruptions, tsunamis and tornadoes, the UAV needs a shorter flight time to scan the area. Therefore, the O-path is the best flight path, and the rectangular path is the next best, followed by the Zig-zag path.

Table 1. The Integrated UAV-based Observer Platform

Use Case	Damage Pattern	Flight Duration	Suggested Flight Pattern
Flood	Distributed	Long	S-Path
Hurricane	Distributed	Long	S-Path
Landslide	Distributed	Long	S-Path
Earthquake	Centralised	Short	1st) O-, 2nd) Rectangular-, and 3rd) Zigzag-path
Volcanic eruption	Centralised	Short	1st) O-, 2nd) Rectangular-, and 3rd) Zigzag-path
Tsunami	Centralised	Short	1st) O-, 2nd) Rectangular-, and 3rd) Zigzag-path
Tornado	Centralised	Short	1st) O-, 2nd) Rectangular-, and 3rd) Zigzag-path

In addition, many studies [8, 14-16] have proposed many high-level optimised UAV flight routes while considering the minimisation of battery consumption. However, the process by which the studies described above determine an optimal route means they do not apply to drones with uncertain geographic conditions on the first flight missions. There is not enough time for this kind of preparation in some emergencies. Identifying a default first-flight route to minimise energy consumption while providing optimal coverage is critical.

On the other hand, many other conditions (natural and experimental) affecting flight status cannot be ignored [17, 18]. Therefore, limiting external influencing factors as much as possible to ensure a more accurate objective evaluation of research is a critical evaluation consideration [19]. Considering the UAV evaluation, the research [20] measured the energy consumption of the UB-ANC UAV flight, which measures when:

1) The straight-line distance is 20m, 40m, 60m, and the speed is 5m/s,
2) The straight-line distance is constant at 40m, and the speed is at 5m/s and 10m/s,
3) For rotation angles of 0°, 45°, 90°, 135°, 180°, the distance is constant 40m and the speed is constant 5m/s.

The comparison of the total energy results for distance, speed, and turn angle was summarised in [13]. Its results show that the greater the distance, the higher the energy consumption. The higher the speed, the less energy is consumed. With the increasing angle, the steering angle makes the drone consume less energy to the maximum.

The research [20] also identified some factors affecting the power consumption of UAVs and investigated their power consumption when performing horizontal movement, vertical movement and hovering. Wind and temperature are External factors that affect a UAV’s power consumption. Different wind directions and speeds can benefit or harm the UAV, and temperature conditions can affect battery consumption and capacity. The intrinsic factors that affect the energy consumption of UAVs are the flight speed and payload. UAVs have three important flight modes: hover, horizontal, and vertical movement. The three kinds of motions have different energy consumption for UAVs. In addition, the weight of the UAV itself, as well as the weight of cameras, sensors, and other accessories, are also constraints on the energy consumption of the UAV.

Second, the classifier is one indispensable tool for developing a detecting system [21, 22]. The fuzzy classifier is popular among various classifiers because it can interpret a trained model [23]. It is worth noting that various EDA-based fuzzy classifiers were proposed for real-time data streams and complex problems [24, 25]. Their advantages make it possible to develop an efficient and intelligent system for the proposed integrated UAV-based observer platform. Its methodology details will be introduced in Section 3.4.

3.0 METHODS AND MATERIAL

The proposed integrated UAV-based observer platform contains four parts: UAV Controller, UAV, Operator, and Computer. Figure 3 shows their working collaboration. It is worth noting that the computer has deployed a new online fuzzy classifier to detect abnormal objectives in the picture stream. According to the two identified objectives in Section 1, this methodology needs to identify the following five parts:

1) UVA device,
2) UAV First Flight Path,
3) Observing zone,
4) online fuzzy classifier,
5) Evaluation method.

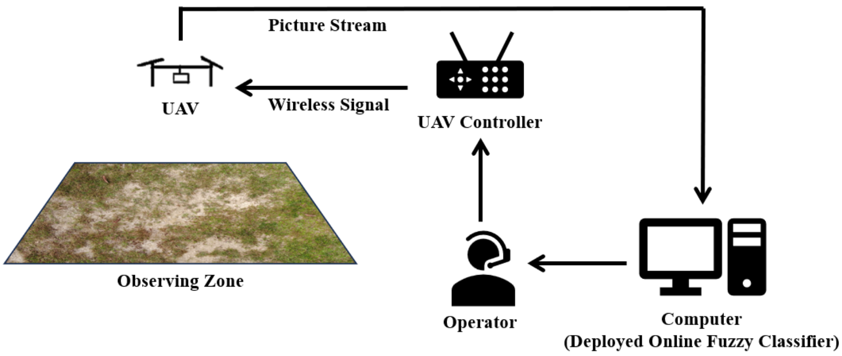

Figure 3. The Proposed Integrated UAV-based Observer Platform

3.1 UAV Device

UAVs are divided into multi-rotor and fixed-wing. Multi-rotor UAVs fly with the fuselage as the centre and 4-8 rotors as powered propellers, while the design of fixed-wing UAVs is similar to that of aeroplanes, with the fuselage as the centre, two wings, and one powered propeller. Both multi-rotor and fixed-wing UAVs have their deployment specifications. Therefore, both have similarities, differences, and advantages and disadvantages. Multicopters have better manoeuvrability than fixed wings because they can take off and land vertically, while fixed wings require a larger takeoff and landing area. Multirotors are 7 to 10 times cheaper in exact specs and mass than fixed wings. The multi-rotor can be folded, and the fixed wing cannot be folded, making it more compact. It is easier to use than a fixed wing and has a high payload capacity. Hence, a multi-rotor UAV equipment, MAVIC AIR (Figure 4), is employed in this research.

Figure 4. Multi-rotor Quadcopter and Fixed-wing UAVs

3.2 UAV First Flight Path

As the reference [12] recommended setting the test area square or rectangular, this research also adopts the same strategy to restrict the test area boundary to a square. The flight path standard requires complete coverage of the entire test area during flight. Meanwhile, to ensure the first route's diversity, simplicity, and practicality, as summarised in Figure 5, the seven UAV flight routes are extended based on the research [11], including circular helix, square helix, zig-zag, S-path, smooth-turn square helix, smooth-turn zig-zag, and smooth-turn S-path. The expansion rules of these paths are based on practical experience and are more convenient to operate. This ensures that they can be easily deployed for emergency missions. Hence, the evaluating experiment will not limit their exact routes. Instead, it will be controlled by an operator's direct control.

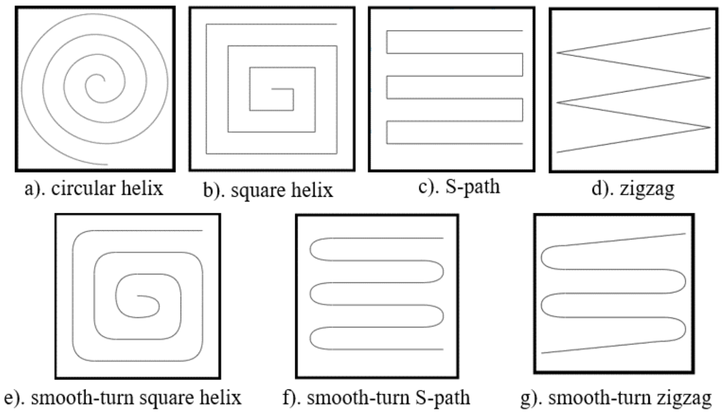

Figure 5. Extended Seven Routes for First Flight Route

3.3 Observing Zone

Testing was conducted through Mission Planner simulations and actual experiments with drone equipment. Figure 6 illustrates the entire testing procedure. First, create a test area for simulation and real experiments. It is recommended that the test area be square or rectangular. Then, plan possible UAV flight routes for the first flight mission. The flight route standard requires complete coverage of the entire test area. The Mission Planner software is used, and the actual experiment uses the DJI Mavic Air with the "Lychee" application.

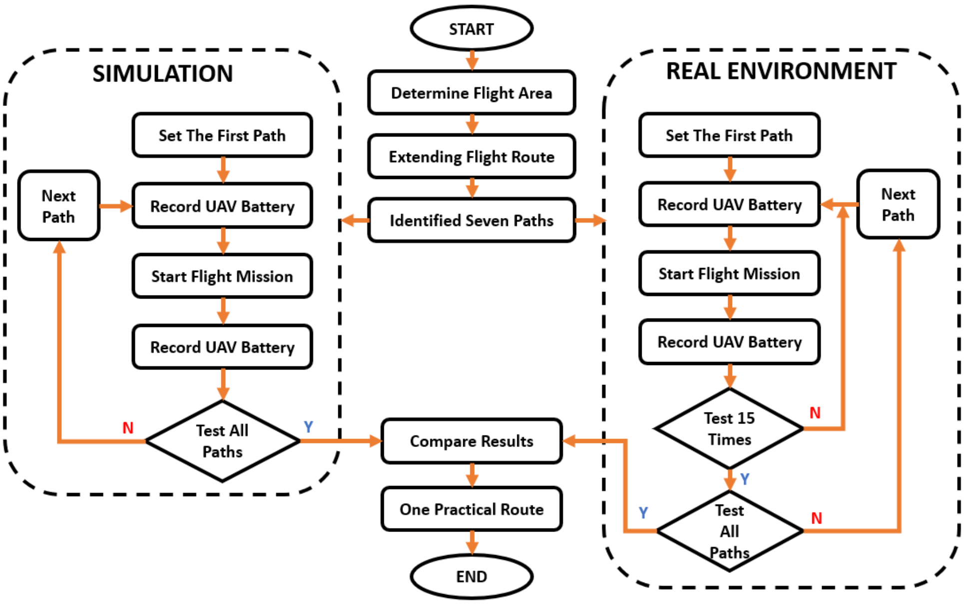

Figure 6. The Overall Procedure of Simulation and Real Experiment

For the simulation, there was only one flight test for each of the seven flight paths. This is because the algorithms in Mission Planner are fixed, and there are no external disturbances in the simulation. Therefore, the results of UAV battery consumption are always accurate. In contrast, the actual test of the UAV unit will be tested 15 times on each route. This is because external disturbances such as wind and temperature can affect the accuracy of the UAV's battery consumption.

Before conducting the research tests, experiment limitations need to be defined to avoid this research being too broad and unfocused. The limitation is as follows:

1) DJI MAVIC AIR is used for a real experiment.
2) Mission Planner is used for simulation.
3) The testing area is set to 210099 m^2.
4) The UAV's flying height is 95m.
5) The UAV's flying speed is 5m/s.
6) The UAV flying test amount for the real experiment is set to 15.
7) The UAV flying test amount for simulation is set to 1.
8) The UAV flying test time for the real experiment is set to 6 p.m.

3.4 Online Fuzzy Classifier-based Observer

EDA technology has been employed frequently to propose online fuzzy classifiers [24-26] because it enables the classifier to operate with high operational efficiency, especially when dealing with high-dimensional data problems. Based on the above advantages, this research will also employ EDA to propose one online classifier for a UAV to observe abnormal objectives. Proposing the EDA-based online fuzzy classifier follows the following five steps:

STEP 1: Identifying Online Observer's Structure

First, the observer should support the online environment when a flying UAV is searching for abnormal objectives. That stresses that the observer has higher speed and efficiency in processing vision information. The EDA-based fuzzy classifier [24, 26, 27] has a natural advantage because it employs no-parameter data clouds to explain data distribution. Therefore, the observer core is the online fuzzy classifier.

Considering the different information in the three-channel colours of an image, this research expands three T0FC as a parallel structure to process different colour channels simultaneously. Due to three parallel structures, a decision fusion maker is required to make the final decision (predicting label).

Last but not least, the vision information is extremely high-dimensional [28], which means various unknown distributions or features will occur. Typical classifiers [19, 29] are weak to process because too many unknown distributions are hard to track, summarise, and explain. For such problems, data augmentation [30] techniques are necessary for the observer. However, original vision information (consisting of continuous images) contains a massive number of high-dimensional vectors. This paper proposes a chunk-searching method to alternate directly with objective detection techniques. This method can save serious computing resources. It is worth noting that employing this method has the belief of the robust online fuzzy classifier in processing high-dimensional information.

At this moment, the final observer's structure could be built, as summarised in Figure 7:

1) flying UAV-based observer is recording video (a picture stream) in real time,
2) a chunk-searching method will collect various smaller image chunks,
3) these chunks will be sent to three classifiers in different colour channels,
4) these chunks will be augmented and sent to the classifier again for training,
5) once unknown chunks come with a requirement for a label, three local decision-makers will process them, the decision fusion maker will decide the final predicted label for an unknown chunk.

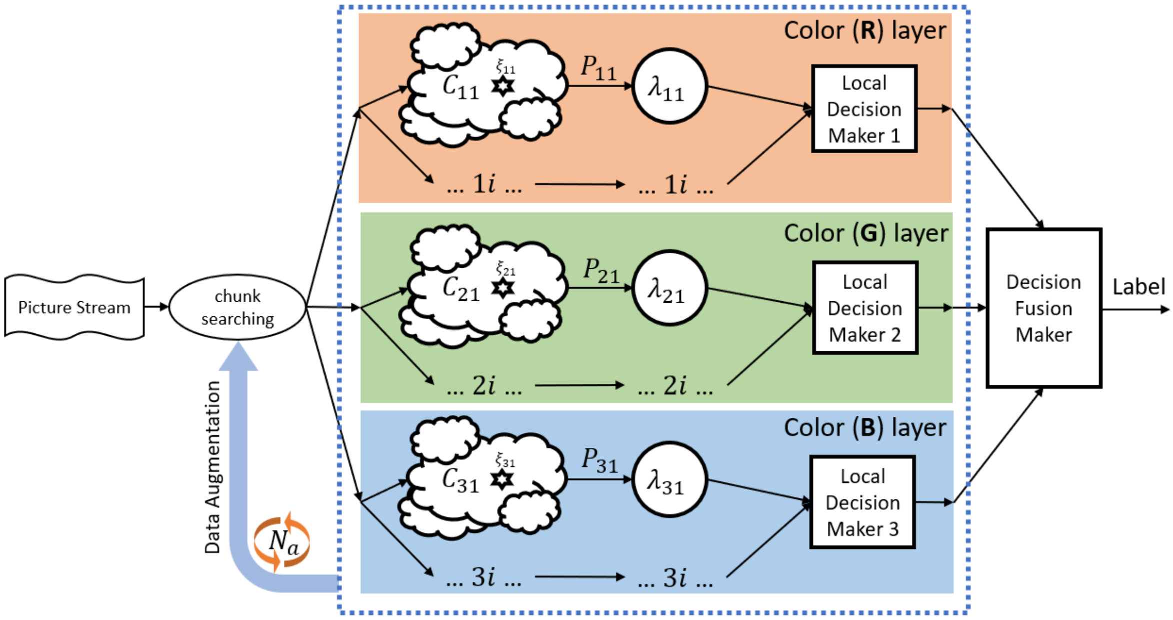

Figure 7. Proposed Online Fuzzy Observer's Structure

STEP 2: Chunk Searching and Augmentation Method

Supposing the operator of the UAV-based observer has noticed one abnormal objective, the observer will hover there and randomly collect some small chunks (squares) of the observing zone, as shown in Figure 8. However, the chunk size must be defined in advance because the proposed observer is not fully automatic. When a fixed flying height is collected, the chunk size can be calculated based on the sizes of the observing image and objective. This paper suggests that the size of chunks is not more than two times the length of one objective. For instance, this paper uses poker as the objective. The chunk size (pixels) is not higher than 1.5 times the length (pixels) of poker.

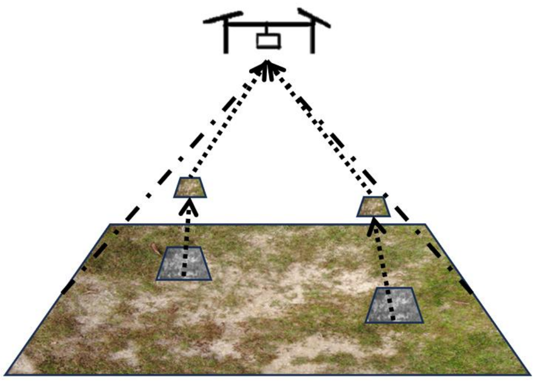

Figure 8. Chunks searching from observing zone

Chunk augmentation will employ two standard traditional methods, including rotation and rescale. The rotation range is set randomly between 0° and 360°. Due to the chunk being square and being rotated, the rescaling value is randomly set higher than one and lower than 1.5. It is worth noting that this research does not augment chunks only once, but a variable (augmenting times, N_a) is given, as Figure 7 shows. This paper suggests $N_a \geq 5$.

STEP 3: Online Fuzzy Classifier

As Figure 7 shows in STEP 1, three fuzzy classifiers will compose one online observer system. They will be trained in three different colour channels. Each classifier's structure is one classic structure [26] and is identified as the following:

$$\begin{cases} RULE_1: IF\big(D = (\xi_{11} \sim X_k)\big)\, THEN(C_1) \\ \vdots \\ RULE_i: IF\big(D = (\xi_{1i} \sim X_k)\big)\, THEN(C_c) \end{cases}, \tag{1}$$

where C means the class label that a fuzzy rule has. D means the similarity ($\sim$) between a prototype (an actual data sample) ξ_r and the current data instance X_k. In EDA, the similarity is defined by the local density value. The local density is followed by Cauchy distribution as the following expression:

$$D(X) = \frac{1}{1 + \frac{\|X - \xi\|^2}{\Psi - \|\Phi\|^2}}, \tag{2}$$

where Φ is the mean of a Data Cloud in a fuzzy rule, and Ψ is the scalar product of the data cloud.

STEP 4: Classifier Learning Machine

The key to learning from data is identifying outlier data that differs from previous data distribution in the cloud. EDA employ global density inequality [24, 26] to resolve this problem. The proposed inequality is expressed as the following:

$$(D_G(\boldsymbol{X}) > max\, D_G(\boldsymbol{\xi}))\ OR\ (D_G(\boldsymbol{X}) < min\, D_G(\boldsymbol{\xi}))\ ; \tag{3}$$

$$\|X_k - \boldsymbol{\xi}\| \leq D(\boldsymbol{X}) * \emptyset_G\ , \tag{4}$$

$$\emptyset_G = \frac{1}{2}\sqrt{2(\Psi_G - \|\boldsymbol{\Phi}_G\|^2)}\ ; \tag{5}$$

where D_G is a global data cloud's density of fuzzy rule, summarising all data samples as a global Cauchy distribution. $\emptyset_G$ is its global spreading radius calculated by Ψ_G and $\boldsymbol{\Phi}_G$ of a global data cloud in a fuzzy rule.

According to the above inequality, a new fuzzy rule will be built once satisfied. Otherwise, a fuzzy rule should be updated based on the current data instance. As the equation expresses, Φ and Ψ are essential for explaining the data density distribution. Based on EDA, the two variables are updated as the following process:

$$N = N + 1\ ; \tag{6}$$

$$\Phi = \frac{N}{N+1}\Phi + \frac{1}{N+1}X\ ; \tag{7}$$

$$\Psi = \frac{N}{N+1}\Psi + \frac{1}{N+1}\|X\|^2\ . \tag{8}$$

After every updating step, the learning machine will update the nearest DC's focal point (ξ) according to the following strategy satisfied or not. The updating strategy is summarised as the following:

$$D(\boldsymbol{X}) \geq D(\xi)\ ; \tag{9}$$

STEP 5: Identifying Decision Maker

As Figure 7 shows, the proposed observer contains two kinds of decision-makers: Local Decision Maker (LDM) and Decision Fusion Maker (DFM). LDM will identify the nearest local Data Cloud to the current data sample with the highest similarity (Local Density Value) in each class. Notably, it does not make any decision on the class label. Once all similarities are received from all fuzzy rules, the DFM will output one predicted label for the current data sample.

The LDM is identified as the following: due to the powerful explaining ability of the Data Cloud among fuzzy rules, one classic decision-making strategy, winner-takes-all, is employed to identify the nearest Data Cloud. The strategy is summarised as follows:

$$M = max(D(X))\ . \tag{10}$$

The DFM is proposed as the following: Once all local maximum similarities (M) are collected from the LDM in each Fuzzy Rule, DFM will normalise them together between 0 and 1. Then, the exponential distribution ($Y = e^{-X}$) [24] is employed for the final decision. Their normalising and deciding zones are illustrated in Figure 9. The decision strategy employed is summarised as follows:

$$LABEL = i = argmax_{L=1,\dots 3; i=1,2}\, e^{-M^{*}{}_{Li}}\,; \tag{11}$$

$$M^{*} = normalizing_{0}^{1}(M)\,. \tag{12}$$

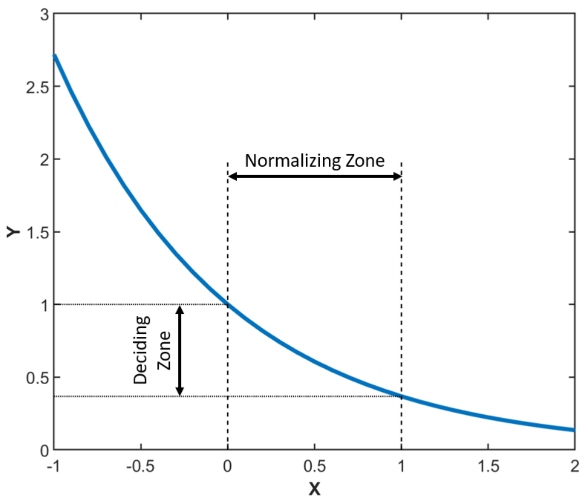

Figure 9. Normalising and Deciding Zone in Exponential Distribution

Code Paragraph	Equation
Initialising **T0FC**	
form the first Fuzzy Rule by $\boldsymbol{X}$;	
FOR $k \rightarrow \infty$	
IF $\boldsymbol{X}_k$ with Label	
IF new Label	
form a new Fuzzy Rule;	
ELSE	
IF condition 1 is satisfied	$Eq.3$
form a new local DC	
ELSE	
IF condition 2 is satisfied	$Eq.4$
update the nearest DC	$Eq.6,7,8$
update focal point of the nearest DC	$Eq.9$
ELSE	
form a new local DC	
END IF	
END IF	
END IF	
ELSE	
calculating all local similarities of $\boldsymbol{X}$	$Eq.2$
identify maximum similarities in each Fuzzy Rule	$Eq.10$
normalising the maximum similarities	$Eq.12$
predicting a Label for $\boldsymbol{X}$	$Eq.11$
END IF	
END FOR	

Figure 10. Online Observer’s Pseudocode

As the last step, the whole online observer's pseudocode can be given as shown in the following Figure 10: when the observer receives the first data sample, as No.2 summarised, it will use the data sample to build three rules in three classifiers for different colour channels, respectively. Then T0FC will go into an infinity loop from No.3 to No.25. If the current data sample has a label, T0FC will train itself from No.4 to No.18. Otherwise, T0FC will predict one label to the current data sample by following No.19 to No.24.

3.5 Evaluation method

This paper focuses on two tasks: identifying one optimal first flight route among seven routes and identifying the proposed online observer as effective. Identifying the first flight route is an empirical process. Hence, this paper will not precisely match them. Instead, this paper will only pay attention to their effect on the battery consumption of UAVs. On the other hand, identifying the real-time performance of the proposed observer requires tracking its accuracy (False and True Accuracies). In sum, this paper will check the performance on the following conditions:

1) Identify a first flight route with minimised battery consumption,
2) Identify the accuracy of the proposed online observer is over 0.9 at least,
3) Identify the real-time performance of the proposed online observer, which can converge by itself.

4.0 RESULTS AND DISCUSSION

4.1 Simulation Experiment

The simulation is undertaken using Mission Planner software. First, open the simulation section and choose the UAV multi-rotor as the model, as shown in Figure 11. Then, open the flight plan and determine the UAV flying area to be $210099m^2$ by putting the polygon point shown in Figure 12. Next, plot the seven UAV flight paths into the simulation area.

Figure 11. Open simulation and choose multi-rotor

Figure 12. Set the simulation area using a polygon point

The Round spiral pattern of the UAV's flight path is shown in Figure 13. All the waypoints are set to "spline" mode, allowing the drone to follow the waypoints curvedly. The drone will take off from waypoint 1 to an altitude of 95m, as shown in the upper left corner of Figure 13. When the drone reaches a height of 95m from waypoint 1, it flies horizontally to waypoint 2, then waypoint 3, until waypoint 9. When the drone reaches waypoint 9, it will change the mode to "return home", which is waypoint 1. After the drone returns to waypoint 1, change the mode to Landing. Cells used for circular spiral patterns are reported in mAh. In addition, the procedures and parameters for the circular helix were used for the rest of the path tests, and these routes are all illustrated in Figures 14 to 19, respectively.

Figure 13. Round spiral

Figure 14. S path

Figure 15. S path with smooth turning

Figure 16. Square spiral path

Figure 17. Square spiral with smooth turning

Figure 18. Zig zag path

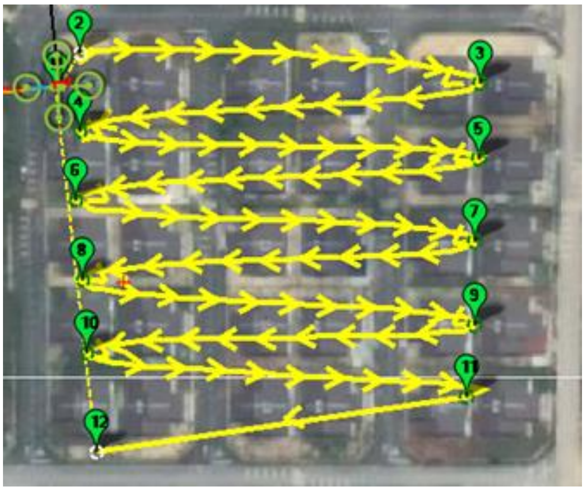

Figure 19. Zig-zag path with smooth turning

In the simulation experiment, the seven UAV flight paths from Figure 13 to 19 will undergo simulation to calculate their battery used in mAh to determine which UAV flight path is ideal for the first flight route.

The simulation result states that the round spiral path consumes 1633mAh, the Square Spiral path consumes 1499mAh, the S path consumes 1679mAh, the Zig Zag path consumes 2637mAh, the Square Spiral with smooth turning consumes 1453mAh, the S path with smooth turning consumes 1606mAh, and Zig Zag path with smooth turning consumes 2370mAh. They have been summarised in Table 2 of Section 4.3.

The results show that the Zig-zag path has the highest battery consumption because every turning 135 degrees takes the highest energy consumption for UAV compared to 45 degrees, 90 degrees, and 180 degrees. Both the S path and S path with smooth turning consume more energy than the Square Spiral path and Square Spiral path with smooth turning. This is because the S path and S path with smooth turning have higher turning amounts than the Square Spiral path and Square Spiral path with smooth turning. The Square Spiral with smooth turning takes the minor energy consumption among the seven paths because it has angular turning, while the Square Spiral has a straight 90-degree turning angle.

4.2 Real Environment Experiment

This experiment was undertaken using DJI Mavic Air. Firstly, switch on the smartphone, DJI UAV, and remote to check the battery. It needs to be fully charged status. Then, connect the smartphone to the DJI remote, turn on the GPS location, and open the ‘litchi’ apps using the smartphone, as shown in Figure 20. Then, take off the drone from the home point to an altitude level of 95m to ensure that there is no blocking disturbance and a clear field of view. The home point location and altitude level must be similar to the simulation.

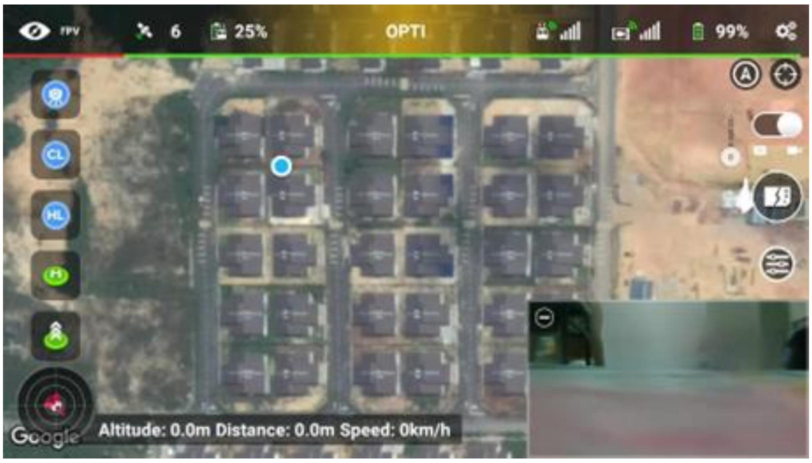

Figure 20. Open ‘litchi’ apps.

After completing the setup, inside the ‘litchi’ apps, open the ‘Set Waypoint’ function, as shown in Figure 21, to set and save waypoints in ‘litchi’ apps according to the simulation for the seven UAV flight paths. Due to the high temperature being a disturbance to UAV battery consumption, the experiment of flying UAV devices is conducted at 6 p.m. as the temperature is lower than in the afternoon. Thus, it creates the slightest disturbance to the UAV battery consumption.

Figure 21. Open the ‘Set Waypoint’ function.

The Round spiral pattern of the UAV flight path is set in Figure 22. All the waypoints are set to ‘curve turn’ mode to make the UAV fly in a curved way following the waypoints. The UAV will take off from HOME (blue dot) to an altitude level of 95m, as shown in the upper left in Figure 23. When the UAV reaches an altitude of 95m, it flies horizontally to waypoint 1, followed by waypoint 2 until waypoint 7. When the UAV reaches waypoint 7, it changes the mode to ‘Return Home’. Once the UAV returns to HOME, it changes the mode to ‘Land’. The battery used in mAh for the round spiral pattern is recorded. Similarly, the same procedure and parameters were used for the Round helix for the rest of the path tests, and these routes are all illustrated in Figures 23 to 28, respectively.

Figure 22. Round Spiral

Figure 23. S path

Figure 24. S path with smooth turning

Figure 25. Square Spiral path

Figure 26. Square spiral with smooth turning

Figure 27. Zig Zag

Figure 28. Zig Zag with smooth turning

The seven UAV flight paths from Figure 22 to 28 undergo a real experiment to determine the battery consumption in mAh and which UAV flight path is ideal for the first flight mission.

The experiment results state that the round spiral path consumes 532mAh, the Square Spiral path consumes 519mAh, the S path consumes 585mAh, the Zig Zag path consumes 817mAh, the Square Spiral with smooth turning consumes 510mAh, the S path with smooth turning consumes 569mAh, and Zig Zag path with smooth turning consumes 798mAh. The results have been summarised in Table 2 of Section 4.3.

The table shows that the Zig Zag path takes the highest battery consumption because every turning angle of this path pattern is 135 degrees. The turning degree of 135 takes the highest energy consumption for the UAV compared to 45 degrees, 90 degrees, and 180 degrees. Both the S path and S path with smooth turning consume more energy than the Square Spiral path and Square Spiral path with smooth turning. This is because the S path and the S path with smooth turning have a higher turning amount than the Square Spiral path and Square Spiral path with smooth turning. The Square Spiral with smooth turning takes the minor energy consumption among the seven paths because it has angular turning while the Square Spiral has a straight 90-degree turning angle.

For a round spiral pattern, UAV battery consumption in simulation is 1633 mAh, while in a real experiment, it is 532 mAh, a difference of 1101 mAh. For the square spiral pattern, UAV battery consumption in simulation is 1499 mAh, while in the real experiment, it is 519 mAh, a difference of 980 mAh. For the S path pattern, UAV battery consumption in simulation is 1679 mAh, while in the real experiment, it is 585 mAh, a 1094 mAh. For the Zig Zag pattern, UAV battery consumption in simulation is 2637 mAh, while in the real experiment, it is 817 mAh, a difference of 1820 mAh. For a square spiral with a smooth turning pattern, UAV battery consumption in simulation is 1453 mAh, while in the real experiment, it is 510 mAh, a difference of 943 mAh. For an S path with a smooth turning pattern, UAV battery consumption in simulation is 1606 mAh, while in the real experiment, it is 569 mAh, a difference of 1037 mAh. For a zig-zag path with smooth turning, UAV battery consumption in simulation is 2370 mAh, while in the real experiment, it is 798 mAh, or 1572 mAh.

In addition, UAV flight tests are limited in simulation and real experiments. In the simulation, the UAV flying speed is fixed to default at 4m/s to 5m/s, and the flying altitude is fixed to default at 95m. Furthermore, wind and temperature are the external disturbances to the UAV during the flight test that affect the accuracy of the result data.

The results revealed that a UAV flying in a square spiral with a smooth turning pattern takes the lowest battery consumption in simulation and real experiments among the seven UAV flight paths. Besides the lowest battery consumption for Square spiral with smooth turning, this flight pattern also fulfils the criteria to cover all the testing areas.

There are three reasons why square spiral with smooth turning for UAVs takes minor battery consumption. First, the total amount of tuning for a Square Spiral with smooth turning is less than that for Zig Zag, Zig Zag with smooth turning, S path, and S path with smooth turning. This is because the UAV needs to decelerate its speed to turn and accelerate to fly in a straight line, and the acceleration and deceleration in flying speed take higher energy consumption than when the UAV flies in a straight line. Therefore, the greater the turning amount of UAV, the higher the energy consumption. Second, the turning for a square spiral with smooth turning is angular, so it takes less energy consumption, while the turning for a square spiral is at a 90-degree angle, which UAV takes higher energy consumption. This is because the speed transformation rate for a UAV to make a turning in angular is lower than turning in 90 degrees. When the speed transformation rate for a UAV is lower, the UAV flies with lower energy consumption. Third, the travelled distance of a UAV in a square spiral with a smooth turning pattern is lower than the round spiral pattern. This is because the lower the travelled distance of the UAV, the lesser the time the UAV is in flying mode, hence the lower the energy consumption of the UAV.

4.3 Energy Consumption Comparison

All values of artificially operation are summarised in Table 2. For a round spiral pattern, UAV battery consumption in simulation is 1633 mAh, while in the real experiment, it is 532 mAh, a difference of 1101 mAh. For the square spiral pattern, UAV battery consumption in simulation is 1499 mAh, while in the real experiment, it is 519 mAh, a difference of 980 mAh. For the S path pattern, UAV battery consumption in simulation is 1679 mAh, while in the real experiment, it is 585 mAh, a 1094 mAh. For the Zig Zag pattern, UAV battery consumption in simulation is 2637 mAh, while in the real experiment, it is 817 mAh, a difference of 1820 mAh. For a square spiral with a smooth turning pattern, UAV battery consumption in simulation is 1453 mAh, while in the real experiment, it is 510 mAh, a difference of 943 mAh. For an S path with a smooth turning pattern, UAV battery consumption in simulation is 1606 mAh, while in the real experiment, it is 569 mAh, a difference of 1037 mAh. For a zig-zag path with smooth turning, UAV battery consumption in simulation is 2370 mAh, while in the real experiment, it is 798 mAh, or 1572 mAh.

Table 2. Battery consumption in simulation and real experiment

UAV Flight path	Battery consumption in Simulation	Battery consumption in Real Experiment
Round Spiral	1633	532
Square Spiral	1499	519
S path	1679	585
Zig Zag path	2637	817
Square spiral smooth turn	**1453**	**510**
S path smooth turn	1606	569
Zig Zag smooth turn	2370	798

In addition, UAV flight tests are limited in simulation and real experiments. In the simulation, the UAV flying speed is fixed to default at 4m/s to 5m/s, and the flying altitude is fixed to default at 95m. Furthermore, wind and temperature are the external disturbances to the UAV during the flight test that affect the accuracy of the result data.

The results revealed that a UAV flying in a square spiral with a smooth turning pattern takes the lowest battery consumption in simulation and real experiments among the seven UAV flight paths. Besides the lowest battery consumption for Square spiral with smooth turning, this flight pattern also fulfils the criteria to cover all the testing areas.

There are three reasons why square spiral with smooth turning for UAVs takes minor battery consumption. First, the total amount of tuning for a Square Spiral with smooth turning is less than that for Zig Zag, Zig Zag with smooth turning, S path, and S path with smooth turning. This is because the UAV needs to decelerate its speed to turn and accelerate to fly in a straight line, and the acceleration and deceleration in flying speed take higher energy consumption than when the UAV flies in a straight line. Therefore, the greater the turning amount of UAV, the higher the energy consumption. Second, the turning for a square spiral with smooth turning is angular, so it takes less energy consumption, while the turning for a square spiral is at a 90-degree angle, which UAV takes higher energy consumption. This is because the speed transformation rate for a UAV to make a turning in angular is lower than turning in 90 degrees. When the speed transformation rate for a UAV is lower, the UAV flies with lower energy consumption. Third, the travelled distance of a UAV in a square spiral with a smooth turning pattern is lower than the round spiral pattern. This is because the lower the travelled distance of the UAV, the lesser the time the UAV is in flying mode, hence the lower the energy consumption of the UAV.

4.4 Observer Performance Investigation

In the real flying experiment, the UAV randomly collected 1680 chunks (including 143 chunks capturing abnormal objectives (poker) and 1538 chunks covering grassy, sandy, and mixed land texture) from the observing zone. In order to save more computing resources for online system speed, this paper did not expand all chunks but only expanded 143 chunks (True Chunks) covering abnormal objectives or partial objectives. The statistic of chunk augmentation is summarised in Figure 29.

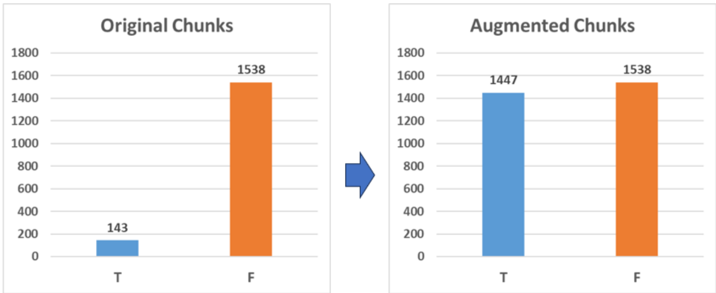

Figure 29. Distribution of Original Chunks and Augmented Chunks

The observer's real-time performance (including the True Accuracy plot in Red, False Accuracy plot in Yellow, and Global Accuracy plot in Blue) is recorded in Figure 30. The results proved that the online observer has high detecting performance and can guarantee its converging ability over more chunks collected in real time. In contrast to the proposed online observer, this research also recorded the real-time performance of a single classifier without data augmentation, as plotted in Black in Figure 30. The result revealed:

1) Augmentation can support a classifier to converge itself as soon as possible,
2) The colour channels-based classifier can have higher performance and robustness.

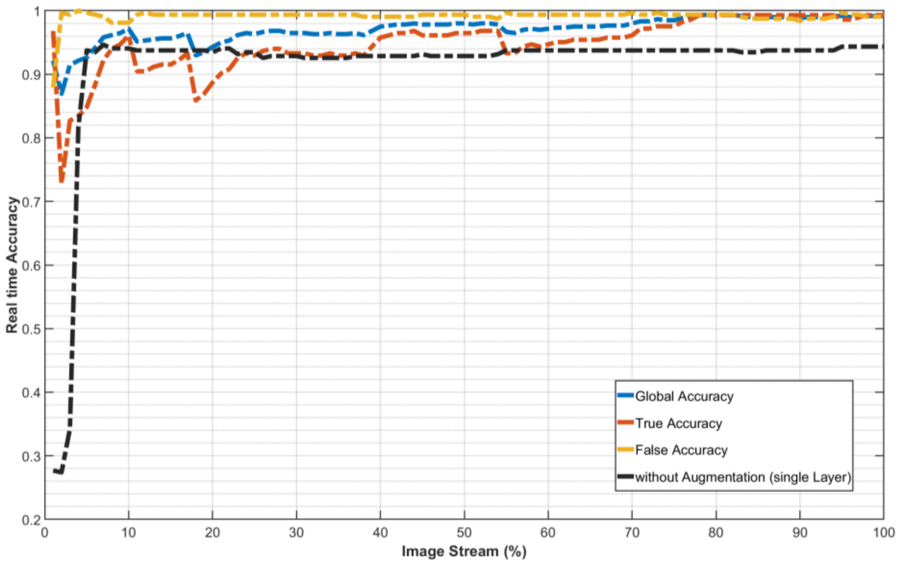

Figure 30. Online Observer's Realtime Performance (Accuracy)

As the last step, this paper explored the observer inside. All of the observer's fuzzy rules are illustrated in Figure 31. Three colour blocks mean three colour channels. Each block contains two trained rules with different class labels (the upper rule is False class, and the lower rule is True class). These rules are combined with captured chunks containing multiple local prototypes and one global cloud. These also support the idea that the proposed online observer performs excellently in system interpretability.

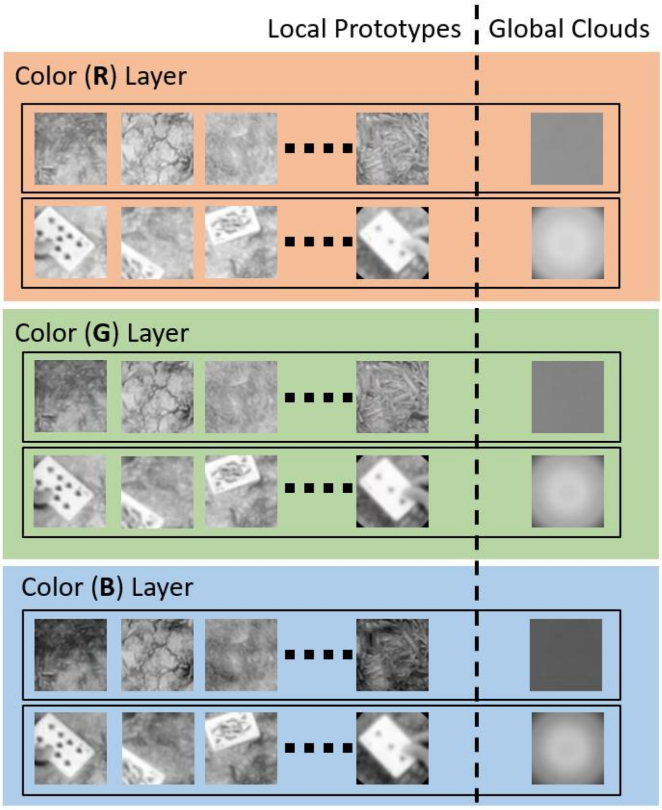

Figure 31. The Prototypes and Clouds in Trained Fuzzy Rule

5.0 CONCLUSIONS

This research artificially evaluates seven practical UAV's first flight routes through simulation and real-world experiments to determine the optimal UAV first flight route. All seven flight paths route the fundamental criteria: maximise area coverage. The simulation and real test results showed that the UAV flies in a square spiral with smooth turn mode and consumes the least power. It has less steering than the S-Path, Smooth-Steering S-Path, Zig Zag Path, and Smooth-Steering Zig Zag Path. The fewer turns, the less energy the drone expands, as turning from a straight flight requires a speed transition, slowing down before and accelerating after the turn. This change in speed causes the drone to use more energy than flying in a straight line. Second, it travels less than a circular spiral path. The shorter the flight distance, the less energy the drone consumes. Third, it applies curved turns, while the square spiral path applies straight 90-degree turns. Hence, as an optimal UAV's first flight route, a square spiral with a smooth turn can quickly be deployed to a UAV in an emergency, and the UAV will save more battery energy.

On the other hand, one new colour channel-based fuzzy classifier is proposed and hybridised to the inside of the online observer. The proposed integrated observer can support UAVs in detecting abnormal objectives when flying. Also, its performance proved to have higher real-time accuracy and higher robustness (converging ability). Most importantly, this integrated observer is interpretable. This paper also reveals a few future works: a more powerful Decision Fusion Maker, higher efficiency image preprocessing techniques, refining classifier techniques.

ACKNOWLEDGEMENTS

The authors thank UMP for funding this research work under an internal grant RDU190394.

AUTHOR CONTRIBUTION

Wan Isni Sofiah Wan Din (Conceptualization, Supervision, Project Administration, Funding Acquisition),

Loo Chen Wei (UAV Flying Experiment, Software, Data Collection), Wenhao Chen (Methodology of Online Fuzzy Classifier-based Observer; Coding; Writing - original draft),

Azlee Zabidi (Funding Acquisition; Manuscript Evaluation).

CONFLICT OF INTEREST

The authors declare no conflicts of interest.

REFERENCES

[1] P. Jana, and D. Jana, "AutoDrone: Shortest Optimised Obstacle-Free Path Planning for Autonomous Drones," In Proceedings of International Conference on Computational Intelligence, Data Science and Cloud Computing: IEM-ICDC 2021, pp. 3-15, 2021.

[2] Z. Rizman et al., “Development of hybrid drone (HyDro) for surveillance application,” Journal of Fundamental and Applied Sciences, vol. 10, no. 1S, pp. 816-823, 2018.

[3] Z. Liu, and R. Sengupta, "An energy-based flight planning system for unmanned traffic management," In 2017 Annual IEEE International Systems Conference (SysCon), pp. 1-7, 2017.

[4] W. Y. Leong, J. H. Chuah, and T. B. Tuan, The Nine Pillars of Technologies for Industry 4.0: Institution of Engineering and Technology, 2020.

[5] M. A. Rahim et al., "A framework of iot-enabled vehicular noise intensity monitoring system for smart city," In Advances in Robotics, Automation and Data Analytics: Selected Papers from ICITES 2020, pp. 194-205, 2021.

[6] U. Rochayati et al., "IoT Enabled Ventilator Monitoring System for Covid-19 Patients," Journal of Physics: Conference Series, p. 012035, 2021.

[7] A. Thibbotuwawa et al., "Energy consumption in unmanned aerial vehicles: A review of energy consumption models and their relation to the UAV routing," In Information Systems Architecture and Technology: Proceedings of 39th International Conference on Information Systems Architecture and Technology–ISAT 2018: Part II, pp. 173-184, 2019.

[8] Y. Li, and M. Liu, “Path Planning of Electric VTOL UAV Considering Minimum Energy Consumption in Urban Areas,” Sustainability, vol. 14, no. 20, pp. 13421, 2022.

[9] P. Angelov, X. Gu, and D. Kangin, “Empirical data analytics,” International Journal of Intelligent Systems, vol. 32, no. 12, pp. 1261-1284, 2017.

[10] P. P. Angelov, X. Gu, and J. C. Principe, “Autonomous learning multimodel systems from data streams,” IEEE Transactions on Fuzzy Systems, vol. 26, no. 4, pp. 2213-2224, 2017.

[11] J. Modares et al., "Ub-anc planner: Energy efficient coverage path planning with multiple drones," In 2017 IEEE International Conference on Robotics and Automation (ICRA), pp. 6182-6189, 2017.

[12] E. Christy et al., "Optimum UAV flying path for device-to-device communications in disaster area," In 2017 International Conference on Signals and Systems (ICSigSys), pp. 318-322, 2017.

[13] S. Rashed, and M. Soyturk, "Effects of UAV mobility patterns on data collection in wireless sensor networks," In 2015 IEEE International Conference on Communication, Networks and Satellite (COMNESTAT), pp. 74-79, 2015.

[14] S. K. Debnath, R. Omar, and N. B. A. Latip, “A review on energy efficient path planning algorithms for unmanned air vehicles,” Computational Science and Technology, pp. 523-532, 2019.

[15] Y. Xu, and C. Che, "A brief review of the intelligent algorithm for traveling salesman problem in UAV route planning," In 2019 IEEE 9th International Conference on Electronics Information and Emergency Communication (ICEIEC), pp. 1-7, 2019.

[16] D. Jung, and P. Tsiotras, “On-line path generation for unmanned aerial vehicles using B-spline path templates,” Journal of Guidance, Control, and Dynamics, vol. 36, no. 6, pp. 1642-1653, 2013.

[17] K. Wu, B. Fan, and X. Zhang, "Trajectory following control of UAVs with wind disturbance," In 2017 36th Chinese Control Conference (CCC), pp. 4993-4997, 2017.

[18] J. Lv et al., "Fuzzy SMC for UAV to resist strong wind with disturbance approximation," In 2018 Ninth International Conference on Intelligent Control and Information Processing (ICICIP), pp. 93-98, 2018.

[19] M. I. Jaya et al., “SIGMA: A Real-Time Soil and Environment Remote Monitoring for Indoor Garden Management,” In Proceedings of Malaysian Technical Universities Conference on Engineering and Technology (MUCET) 2021, pp. 404-405, 2021.

[20] J. Modares, and N. Mastronarde, "UB-ANC Drone: A Flexible Airborne Networking and Communications Testbed," arXiv preprint arXiv:1509.08346, 2015.

[21] Y. Zhou et al., "Building an efficient intrusion detection system based on feature selection and ensemble classifier," Computer Networks, vol. 174, pp. 107247, 2020.

[22] A. Thakkar, and R. Lohiya, "A survey on intrusion detection system: feature selection, model, performance measures, application perspective, challenges, and future research directions," Artificial Intelligence Review, vol. 55, no. 1, pp. 453-563, 2022.

[23] F. Aghaeipoor, M. M. Javidi, and A. Fernández, "IFC-BD: an interpretable fuzzy classifier for boosting explainable artificial intelligence in big data," IEEE Transactions on Fuzzy Systems, vol. 30, no. 3, pp. 830-840, 2021.

[24] X. Gu, and P. P. Angelov, "Self-organising fuzzy logic classifier," Information Sciences, vol. 447, pp. 36-51, 2018.

[25] X. Gu, P. P. Angelov, and Q. Shen, "Self-Organizing Fuzzy Belief Inference System for Classification," IEEE Transactions on Fuzzy Systems, 2022.

[26] H.-J. Rong et al., "Stability of evolving fuzzy systems based on data clouds," IEEE Transactions on Fuzzy Systems, vol. 26, no. 5, pp. 2774-2784, 2018.

[27] P. Angelov, and R. Yager, "A new type of simplified fuzzy rule-based system," International Journal of General Systems, vol. 41, no. 2, pp. 163-185, 2012.

[28] M. Soni, and M. A. Shnan, "Scalable Neural Network Algorithms for High Dimensional Data," Mesopotamian Journal of Big Data, vol. 2023, pp. 1-11, 2023.

[29] C. Peng, and Q. Cheng, "Discriminative ridge machine: A classifier for high-dimensional data or imbalanced data," IEEE Transactions on Neural Networks and Learning Systems, vol. 32, no. 6, pp. 2595-2609, 2020.

[30] K. Maharana, S. Mondal, and B. Nemade, "A review: Data pre-processing and data augmentation techniques," Global Transitions Proceedings, vol. 3, no. 1, pp. 91-99, 2022.